

# Cosmic Censorship Upheld in Spheroidal Collapse of Collisionless Matter

William E. East

*Perimeter Institute for Theoretical Physics, Waterloo, Ontario N2L 2Y5, Canada*

We study the collapse of spheroidal configurations of collisionless particles in full general relativity. This setup was originally considered by Shapiro and Teukolsky (1991), where it was found that prolate configurations with a sufficiently large semimajor axis gave rise to diverging curvature, but no apparent horizon. This was taken as evidence for the formation of a naked singularity, in violation of cosmic censorship. We revisit such configurations using different coordinates/slicing, and considering a range of values for the semimajor axis and eccentricity of the initial matter distribution, and find that the final state in all cases studied is a black hole plus gravitational radiation. Though initially distorted, the proper circumferences of the apparent horizons that are found do not significantly exceed the hoop conjecture bound. Configurations with a larger semimajor axis can produce strong gravitational radiation, with luminosities up to  $P_{\text{GW}} \sim 2 \times 10^{-3} c^5/G$ .

*Introduction.*—Unhalted, gravitational collapse in Einstein’s theory of general relativity will lead to the formation of singularities where the theory breaks down. Remarkably, it is conjectured that if one excludes regions hidden from far away observers by black hole horizons, Einstein’s theory generically retains its ability to predict the evolution of spacetime. This behavior is referred to as cosmic censorship [1]. (Here, we refer specifically to the *weak* cosmic censorship conjecture.) Violations of cosmic censorship have been shown to occur in the fine-tuned configurations of critical collapse [2], as well as in spacetimes with dimension higher than four [3–5]. However, for more generic initial data in 3+1 dimensions, cosmic censorship has shown to hold in the numerous cases where it has been studied [6].

One possible exception to cosmic censorship is the work of Shapiro and Teukolsky [7] following the collapse of prolate configurations of collisionless particles. In that work, one configuration was found to exhibit a blowup in the spacetime curvature in two spindle regions lying *outside* the collapsing matter, an indication this was not due to just a shell crossing singularity in the matter.<sup>1</sup> No apparent horizon was found before the simulation became unreliable and could no longer be evolved, and this, along with the lack of turn around of null geodesics in the vicinity of the blowup, was taken as evidence that this was a naked

singularity, in violation of cosmic censorship. However, since the calculation could not be continued past the blowup, the possibility of the spacetime containing an event horizon that would hide the final stages of gravitational collapse was not conclusively ruled out. In particular, the absence of an apparent horizon in some gauge does not rule out an event horizon. In fact, one can slice a Schwarzschild spacetime in a way that approaches the singularity without containing outer trapped surfaces [8].

The study of such prolate configurations as candidates for violating cosmic censorship was motivated by Thorne’s hoop conjecture [9]. Though lacking a precise formulation, the hoop conjecture roughly states that a black hole will form if and only if some mass  $M$  can be localized in a region whose circumference in every direction satisfies  $\mathcal{C} \lesssim 4\pi M$ . (Here and throughout we use geometric units with  $G = c = 1$ .) For example, the collapse of an infinite cylindrical distribution of matter will not form a black hole (but will form a singularity) [9]. The hoop conjecture can be violated in the presence of negative energy, for example, by cylindrical black holes in anti-de Sitter spacetimes [10, 11], or due to a scalar field with negative potential [12], where arbitrarily elongated black holes can be formed, but seems to be robust otherwise. Hence the motivation to study the collapse of very prolate distributions of matter which (at least initially) lie outside the hoop conjecture bound to form a black hole [13]. (See Ref. [14] for an analytic proof of black hole formation in a spherical symmetric collisionless matter configuration.)

Despite follow-up work by numerous authors, including relaxing the requirement of axisymmetry and using higher resolution [15, 16], utilizing excision to the causal future of the curvature blowup [17], and

---

<sup>1</sup>A formal statement of the cosmic censorship conjecture requires some “suitability” condition be placed on the matter fields, which could exclude singularities such as fluid shocks or matter shell crossings that could occur even without gravity [6]. Here, following [7], we consider collisionless matter, which can develop caustics, but do not consider such caustics as violations of cosmic censorship.

extending to 5 dimensional spacetimes [18], the question of whether the configurations studied in Ref. [7] violate cosmic censorship has remained unanswered. Here, we revisit the problem, using somewhat different methods that allow us to rescue cosmic censorship and determine the ultimate fate of such spacetimes. We show that the final state is in fact a black hole with, in some cases significant, gravitational radiation.

*Methodology.*—We consider the same family of initial conditions as in Ref. [7], consisting of a prolate spheroidal distribution of collisionless matter, initially at rest, that is axisymmetric and has no angular momentum. This family is parameterized by a semimajor axis length  $b$  (in units of the total mass  $M$ ), and eccentricity  $e = \sqrt{1 - a^2/b^2}$  (where  $a$  is in the equatorial radius). In the Newtonian limit, the spheroids have homogeneous density. At  $t = 0$ , the spatial metric is conformally flat  $\gamma_{ij} = \Psi^4 \delta_{ij}$  and the extrinsic curvature is zero  $K_{ij} = 0$ . See Refs. [13, 16] for further details on the initial data.

In this work, we focus on very prolate cases. In Ref. [7], the cases considered were  $e = 0.9$  with  $b/M = 2$  (prompt collapse to a black hole) and  $b/M = 10$  (candidate for cosmic censorship violation). Here we consider a number of cases with  $e = 0.9$  and  $2 \leq b/M \leq 20$ . We also consider one case with larger eccentricity, namely  $b/M = 10$  with  $e = 0.95$ .

We evolve the Einstein-Vlasov equations describing a distribution of collisionless matter coupled to gravity using the methods of Ref. [19] for evolving massive particles. For gauge conditions at  $t = 0$ , we choose the lapse to be  $\alpha = \Psi^{-4}$  and the shift to be zero  $\beta^i = 0$ . However, we carry out the initial part of the evolution in harmonic gauge. Around the time of collapse, we transition to a damped harmonic gauge [20, 21] (specifically the  $p = 1/4$  version used in Ref. [22]), which we find helps control the strong oscillations in the coordinate shape of the black hole as it settles down. In contrast, in Ref. [7], maximal slicing and isotropic spatial coordinates were used.

We search for apparent horizons—outermost marginally outer trapped surfaces—using a flow method [23]. Once found, we track the evolution of the horizon, measuring several properties including its area—from which a mass  $M_{\text{BH}}$  can be calculated—and its proper circumferences in the polar and equatorial directions,  $\mathcal{C}_p$  and  $\mathcal{C}_{\text{eq}}$ . In the following, we use black hole to refer to the apparent horizon, though for all cases we track the apparent horizon to sufficiently late times that it should become a good approximation for a time slice of the event horizon. The gravitational radiation is measured by calculating the Newman-

Penrose scalar  $\psi_4$ . We also compute the Kretschmann scalar, obtained from contracting the Riemann tensor with itself  $I = R^{abcd}R_{abcd}$ , as well as the matter density, computed from the stress-energy tensor  $\rho = -T^a_a$ .

We restrict to axisymmetry, which allows us to use a computational domain with two spatial dimensions. Most results presented below are obtained using  $N = 1.6 \times 10^6$  particles and an adaptive mesh refinement simulation grid where the finest resolution is  $dx \approx 0.02M$  (for  $b/M \leq 12$  and  $e \leq 0.9$ ) or  $dx \approx 0.01M$  (otherwise). For select cases, we also perform resolution studies to establish convergence using  $0.75\times$  and  $1.5\times$  the grid resolution, and  $0.75^4\times$  and  $1.5^4\times$  as many particles. Details on numerical convergence can be found in the appendix.

*Results.*—Our main result is that we are able to evolve all cases considered here until they settle towards a final state, which we find to be a black hole containing all the matter, along with gravitational radiation. Configurations with smaller values of  $b$  (or larger values of eccentricity, in the case with  $e = 0.95$ ) form black holes more promptly, while those with larger values take longer to collapse—both perpendicular to the symmetry axis, and along the symmetry axis. In Fig. 1, we show the polar and equatorial circumferences of the apparent horizon, beginning when one is first found, for a number of cases. The matter configuration has collapsed sufficiently that the values are not more than  $\sim 25\%$  above  $4\pi M_{\text{BH}}$ , and thus not in serious violation of the approximate inequality of the hoop conjecture. (Though we note that, since our horizon finding algorithm relies on having a sufficiently good guess for the shape, we cannot exclude the existence of a more distorted horizon at earlier times.) After formation, the horizons then exhibit damped oscillations between being prolate and oblate as they ring down towards a stationary state.

All the matter ends up in the black hole for every case studied here. However, a non-negligible amount of energy is radiated away in gravitational radiation. In Fig. 2, we show the gravitational wave power for select cases. The power peaks around the time of black hole formation—reaching as high as  $P_{\text{GW}} \sim 0.002$  in some cases—and then dies away exponentially, again showing the characteristic quasinormal mode ringing.

We also show the total energy in gravitational radiation as function of the semimajor axis length in Fig. 3. Cases with smaller values of  $b/M$  are already close to being black holes at the initial time and do not emit significant radiation. For  $e = 0.9$ , this is maximized at  $b/M \sim 12\text{--}14$ , with  $E_{\text{GW}} \sim 0.015M$ . A similar amount of energy is radiated for  $b = 10$

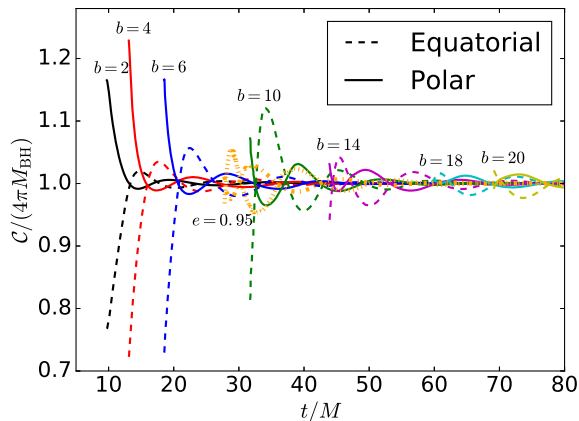


FIG. 1. The polar (solid lines) and equatorial (dashed lines) proper circumferences of the apparent horizons found for various values of the semimajor axis length  $b$  (in units of the total mass). The circumference is normalized by  $4\pi M_{\text{BH}}$ , where  $M_{\text{BH}}$  is the mass of the apparent horizon, to indicate the relation to the hoop conjecture bound. All curves are for initial data with  $e = 0.9$ , except for the dotted (orange) curves which correspond to  $e = 0.95$  and  $b = 10$ .

and  $e = 0.95$ . The difference from the total mass  $M - E_{\text{GW}}$  matches the measured mass of the black hole at late times to better than 0.2% for all cases. The amount of gravitational radiation is significant for an axisymmetric spacetime. For comparison, an equal mass head-on collision of two black holes falling from rest releases 0.06% in gravitational radiation [24], while an ultrarelativistic collision releases 15% of the total mass in gravitational waves, and has a peak luminosity of  $P_{\text{GW}} \sim 0.01$  [22, 25].

Most of the gravitational wave energy is due to the  $\ell = 2$  angular component, but in Fig. 3, we also show the subdominant contributions from the  $\ell = 4$  and 6 components. (The odd  $\ell$  components are suppressed by the symmetry of the initial data, though we do not explicitly enforce the equatorial symmetry in the placement of particles, nor during evolution.)

Focusing on the  $b/M = 10$ ,  $e = 0.9$  case considered in Ref. [7], we also find a blowup in the curvature around the same time. As shown in Fig. 4, the maximum value obtained at blowup increases with resolution. However, in contrast to Ref. [7], we find that the maximum in  $I$  always occur in a region where the matter density is nonzero (this was also found in Ref. [16]), and in fact tracks the blowup in density, as shown in Fig. 4. This indicates that this is just due to

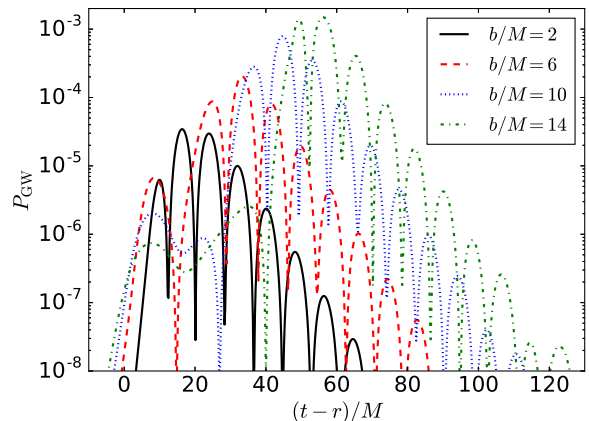


FIG. 2. The gravitational wave power as a function of time for cases with various values of the semimajor axis and  $e = 0.9$ .

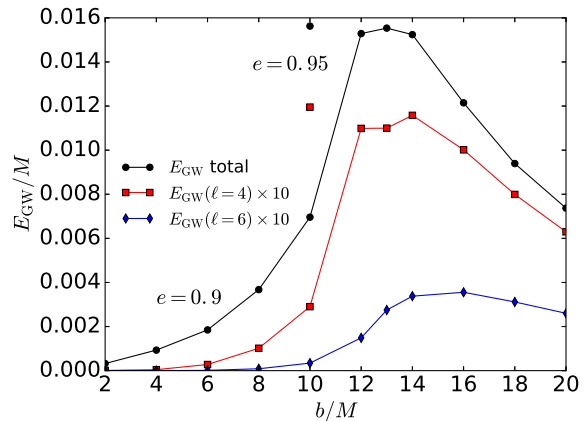


FIG. 3. The total energy emitted in gravitational waves as a function of the semimajor axis  $b$ . The energy is predominantly due to an  $\ell = 2$  component, but we also show the amount in the  $\ell = 4$  and  $\ell = 6$  components, scaled up by a factor of 10 to be visible on the graph. The points connected by lines correspond to  $e = 0.9$ , while the two unconnected points above correspond to  $e = 0.95$ .

the development of caustics in the matter (see, e.g., Ref. [26]).

This is further illustrated in Fig. 5 where we show snapshots of both the matter density and curvature. By integrating null geodesics outward from the caustic to the wave zone, we have explicitly checked that the caustic is “visible” at null infinity. We are able to con-

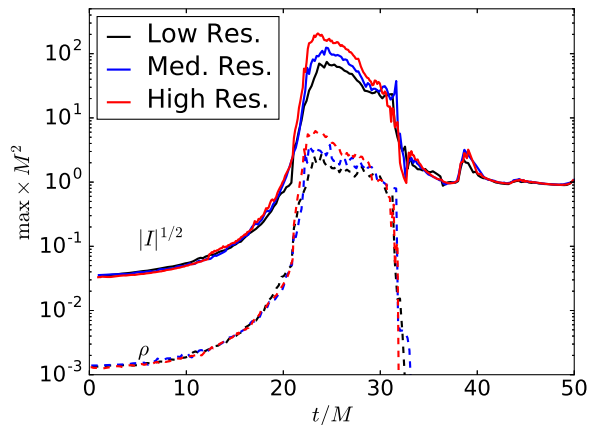


FIG. 4. The maximum value of the particle density (dashed lines) and  $|I|^{1/2}$  (solid lines) as a function of time (both in units of  $1/M^2$ ), for  $b/M = 10$  and  $e = 0.9$  and three different resolutions. At around  $t/M = 30$  an apparent horizon is found, the interior of which is excluded from this calculation.

tinue the calculation past the formation of the caustic (which is mild, e.g., compared to the singularity associated with trapped surfaces). The matter continues rapidly collapsing, and a short time later an apparent horizon is found which envelops all the matter and the region of higher curvature. The curvature outside quickly approaches the value of an isolated black hole.

*Conclusion.*—We have followed the relativistic collapse of very prolate spheroidal configurations of matter, revisiting a scenario originally studied in Ref. [7], and put forth as evidence against cosmic censorship. With our different choice of slicing and coordinates, we do not find a blowup of curvature peaked outside the matter region as in Ref. [7], and we are able to follow the evolution through to the asymptotic end state. We see that a black hole does form, swallowing the matter, and censoring the interior singularity.

The original motivation for investigating this scenario for possible violations of cosmic censorship was that it seemingly pitted the hoop conjecture, which dictates that sufficiently elongated matter configurations should not form black hole horizons, against the generic tendency of unhalting relativistic collapse to form singularities. We find here that the spacetime dynamics unfolds in such a way that, even in the case of collisionless particles, the matter collapses to where it can be surrounded by a horizon that is not too elongated. Thus, neither the hoop conjecture, nor cosmic censorship appear to be violated. This rapid

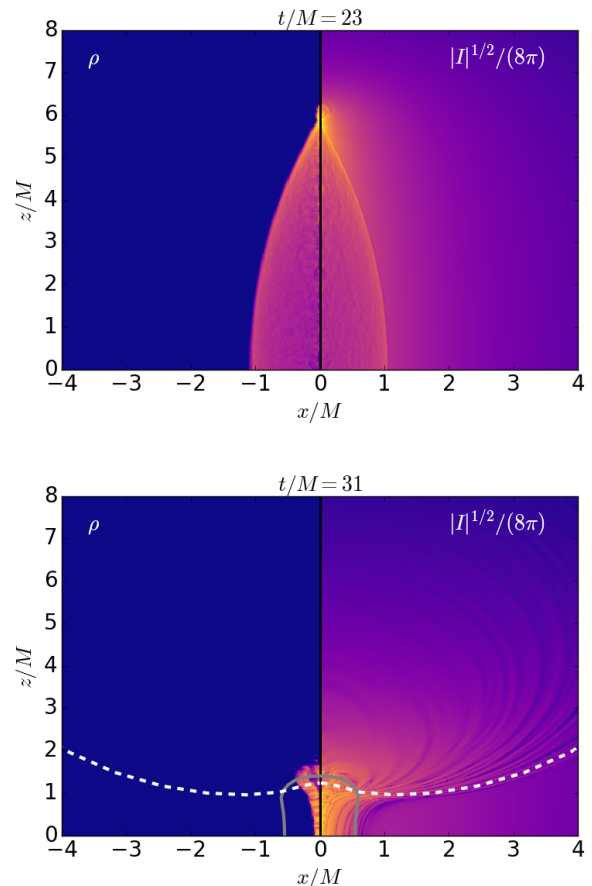


FIG. 5. Snapshots of the particle density (left half) and  $|I|^{1/2}/(8\pi)$  (right half), at the approximate times when a caustic first forms (top) and when an apparent horizon is first found (indicated by the gray curve; bottom) for  $b/M = 10$  and  $e = 0.9$ . The color scale is logarithmic from  $2 \times 10^{-4}$  to 2 in units of  $1/M^2$ . The dashed white curve in the bottom panel represents the position of a set of null geodesics spreading out in all directions from the point of maximum density and curvature in the top panel.

and violent collapse does, however, leave its imprint in the strong gravitational radiation, which for some cases is comparable to a quasicircular binary black hole merger in peak luminosity and the fraction of the total mass of the spacetime.

*Acknowledgements.*—I thank Maria Okounkova and Frans Pretorius for stimulating discussions. This research was supported in part by Perimeter Institute for Theoretical Physics. Research at Perimeter Institute is supported by the Government of Canada through the Department of Innovation, Science and

Economic Development Canada and by the Province of Ontario through the Ministry of Economic Development, Job Creation and Trade. Computational resources were provided by the Symmetry cluster at Perimeter Institute and the Perseus cluster at Princeton University.

---

[1] R. Penrose, Riv. Nuovo Cim. **1**, 252 (1969), [Gen. Rel. Grav.34,1141(2002)].

[2] M. W. Choptuik, Phys. Rev. Lett. **70**, 9 (1993).

[3] L. Lehner and F. Pretorius, Phys. Rev. Lett. **105**, 101102 (2010), arXiv:1006.5960 [hep-th].

[4] P. Figueras, M. Kunesch, and S. Tunyasuvunakool, Phys. Rev. Lett. **116**, 071102 (2016), arXiv:1512.04532 [hep-th].

[5] P. Figueras, M. Kunesch, L. Lehner, and S. Tunyasuvunakool, Phys. Rev. Lett. **118**, 151103 (2017), arXiv:1702.01755 [hep-th].

[6] R. M. Wald, in *Black Holes, Gravitational Radiation and the Universe: Essays in Honor of C. V. Vishveshwara* (1997) pp. 69–85, arXiv:gr-qc/9710068 [gr-qc].

[7] S. L. Shapiro and S. A. Teukolsky, Phys. Rev. Lett. **66**, 994 (1991).

[8] R. M. Wald and V. Iyer, Phys. Rev. **D44**, R3719 (1991).

[9] K. S. Thorne, in *Magic Without Magic: John Archibald Wheeler*, edited by J. Klauder (Freeman, San Francisco, 1972) p. 231.

[10] J. P. S. Lemos, Phys. Lett. **B353**, 46 (1995), arXiv:gr-qc/9404041 [gr-qc].

[11] J. P. S. Lemos, Phys. Rev. **D57**, 4600 (1998), arXiv:gr-qc/9709013 [gr-qc].

[12] W. E. East, J. Kearney, B. Shakya, H. Yoo, and K. M. Zurek, Phys. Rev. **D95**, 023526 (2017), [Phys. Rev. D95,023526(2017)], arXiv:1607.00381 [hep-ph].

[13] T. Nakamura, S. L. Shapiro, and S. A. Teukolsky, Phys. Rev. **D38**, 2972 (1988).

[14] H. Andreasson, Annales Henri Poincare **13**, 1511 (2012), arXiv:1201.3510 [gr-qc].

[15] M. Shibata, Prog. Theor. Phys. **101**, 251 (1999).

[16] C.-M. Yoo, T. Harada, and H. Okawa, Class. Quant. Grav. **34**, 105010 (2017), arXiv:1611.07906 [gr-qc].

[17] M. Okounkova, “Numerical tests of cosmic censorship,” (2016), 21st International Conference on General Relativity and Gravitation.

[18] Y. Yamada and H.-a. Shinkai, Phys. Rev. **D83**, 064006 (2011), arXiv:1102.2090 [gr-qc].

[19] F. Pretorius and W. E. East, Phys. Rev. **D98**, 084053 (2018), arXiv:1807.11562 [gr-qc].

[20] L. Lindblom and B. Szilagyi, Phys. Rev. **D80**, 084019 (2009), arXiv:0904.4873 [gr-qc].

[21] M. W. Choptuik and F. Pretorius, Phys. Rev. Lett. **104**, 111101 (2010), arXiv:0908.1780 [gr-qc].

[22] W. E. East and F. Pretorius, Phys. Rev. Lett. **110**, 101101 (2013), arXiv:1210.0443 [gr-qc].

[23] F. Pretorius, Class. Quant. Grav. **22**, 425 (2005), arXiv:gr-qc/0407110 [gr-qc].

[24] U. Sperhake, V. Cardoso, C. D. Ott, E. Schnetter, and H. Witek, Phys. Rev. **D84**, 084038 (2011), arXiv:1105.5391 [gr-qc].

[25] U. Sperhake, V. Cardoso, F. Pretorius, E. Berti, and J. A. Gonzalez, Phys. Rev. Lett. **101**, 161101 (2008), arXiv:0806.1738 [gr-qc].

[26] J. T. Giblin, J. B. Mertens, G. D. Starkman, and C. Tian, (2018), arXiv:1810.05203 [astro-ph.CO].

### Numerical convergence

We study the collapse of spheroidal distributions of collisionless particles using the code described in [19]. The massive particles follow geodesics on the evolving spacetime, and contribute to the stress-energy tensor used to evolve Einstein’s equations. Though the metric and geodesics are evolved using fourth order accurate methods, the stress-energy calculation is only second order accurate, which sets the overall accuracy of the solution. We use adaptive mesh refinement, with the grid structures determined by truncation error estimates. When performing a convergence study, we adjust the truncation error threshold to be consistent with the expected second order convergence in the grid resolution and (as described in [19]) increase the number of particles by the fourth power of the increase in the linear resolution.

In Fig. 6, we demonstrate the convergence of the Einstein constraints for an example case with  $b/M = 10$  and  $e = 0.9$ . During the initial and final stages of evolution, the rate of convergence is close to second order, as expected (with the number of particles also increased to give this scaling). Around the time the density blows up due to shell crossing (as described in the main text), the convergence is closer to first order, though this quickly improves as an apparent horizon is found (the interior of which is excluded from this calculation).

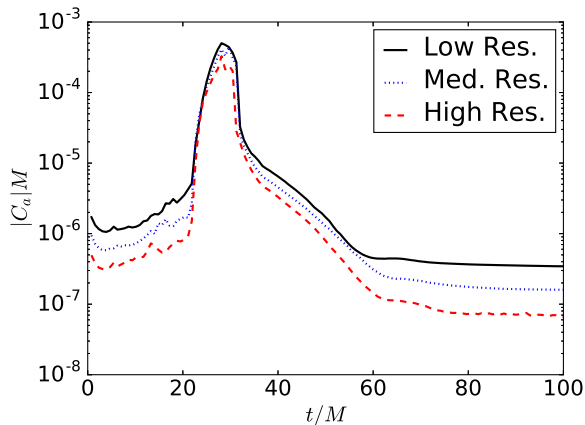


FIG. 6. The L2 norm of the generalized harmonic constraint violation  $C_a = H_a - \square x_a$  (average value in the  $(x, y) \in [-20M, 20M] \times [0, 20M]$  central portion of the domain) at three resolutions for  $b/M = 10$  and  $e = 0.9$ . In comparison to the low resolution, the grid resolution is  $4/3\times$  and  $2\times$  higher in the medium and high resolutions, respectively. The number of particles is  $(4/3)^4\times$  and  $2^4\times$  higher.

Comparing the total energy in gravitational waves for the different resolutions in this case, we estimate that the error in the dominant  $\ell = 2$  contribution is sub-percent for the medium resolution. The error in the very sub-dominant  $\ell = 4$  and  $6$  components (see Fig. 3) is larger, approximately 2% and 30%, respectively.

We show the dependence of the gravitational wave luminosity on resolution for the  $b/M = 16$  case in Fig. 7. The convergence in this quantity is consistent with between first and second order convergence. For this case, this error in the total energy in gravitational waves is larger, approximately 16% for the medium resolution.

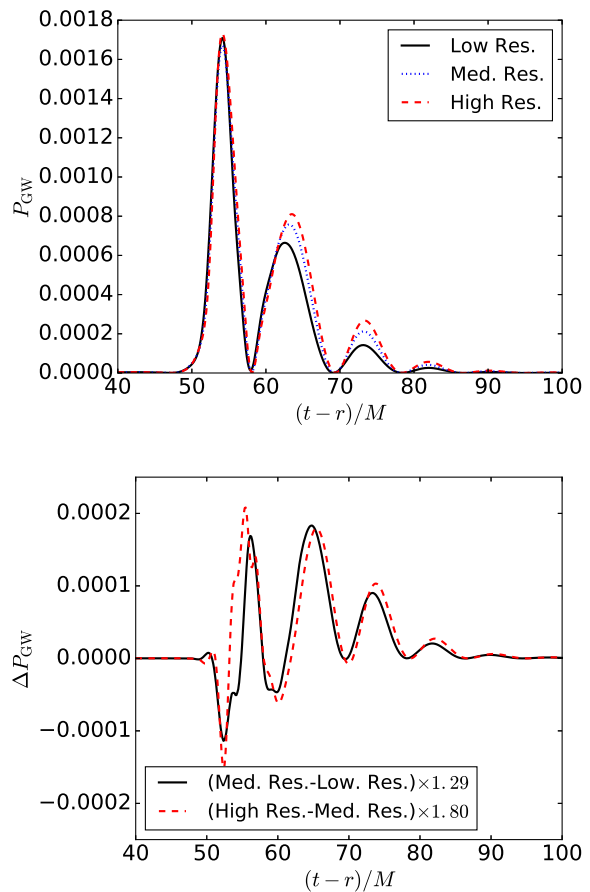


FIG. 7. The top panel shows the gravitational wave luminosity for the  $b/M = 16$  and  $e = 0.9$  case at three resolutions. The bottom panel shows the difference in this quantity between resolutions, scaled assuming second order convergence. The relative grid resolution and number of particles is the same as in Fig. 6.